



Regular Article

Mechanical properties of nanostructured thermoelectric materials α -MgAgSb

Zihang Liu^{a,b}, Weihong Gao^a, Xianfu Meng^a, Xiaobo Li^a, Jun Mao^{b,c}, Yumei Wang^{b,d}, Jing Shuai^b, Wei Cai^a, Zhifeng Ren^{b,*}, Jiehe Sui^{a,*}

^a National Key Laboratory for Precision Hot Processing of Metals, and School of Materials Science and Engineering, Harbin Institute of Technology, Harbin 150001, China

^b Department of Physics and TcSUH, University of Houston, Houston, TX 77204, USA

^c Department of Mechanical Engineering, University of Houston, Houston, TX 77204, USA

^d Beijing National Laboratory for Condensed Matter Physics, Institute of Physics, Chinese Academy of Sciences, Beijing 100190, China

ARTICLE INFO

Article history:

Received 13 July 2016

Accepted 30 August 2016

Available online xxxx

Keywords:

Thermoelectric materials

Mechanical properties

Nanostructure

MgAgSb

ABSTRACT

Mechanical robustness plays an important role in the manufacturing and assembling processes as well as reliable operation for thermoelectric devices. Herein, we first give a detailed study on the mechanical properties of nanostructured α -MgAgSb. The corresponding Young's modulus, nanoindentation hardness, compressive strength, and fracture toughness are 55.0 GPa, 3.3 GPa, 389.6 MPa, and 1.1 MPa m^{1/2}, respectively, which have a close relationship with the intricate microstructure. Compared with other p-type thermoelectric materials, the good mechanical properties of nanostructured α -MgAgSb further highlight the realistic prospect for power generation.

© 2016 Acta Materialia Inc. Published by Elsevier Ltd. All rights reserved.

Due to the high energy demand and critical environmental crisis in the 21st century, thermoelectric power generation (TEG) has received renewed attention as a clean energy conversion technology for waste heat recovery [1–3]. The conversion efficiency is mainly determined by thermoelectric figure of merit ZT , $ZT = S^2\sigma T / (\kappa_{lat} + \kappa_{ele})$, where S , σ , T , κ_{lat} , and κ_{ele} are the Seebeck coefficient, electrical conductivity, absolute temperature, lattice thermal conductivity, and electronic thermal conductivity, respectively. In practical applications, ZT or efficiency is not the only concern for harvesting energy. Mechanical robustness should be good enough to realize the high TE performance, otherwise the manufacturing and assembling processes as well as reliable operation of TEG devices will be impossible [2]. Poor mechanical properties increase the difficulty of machining and thus lower the yield. Since TE materials usually work under a cyclic temperature gradient, poor mechanical properties may also lead to crack generation and consequently the deteriorated performance under thermal stress. More seriously, the additional severe mechanical vibration may accelerate the failure process of TEG devices in applications such as automobile's waste heat recovery [4]. To date, effort primarily focused on pursuing high ZT via band engineering [5] or nanostructuring [6] while limited thorough studies on the mechanical properties of advanced TE [7–11].

Recently, p-type α -MgAgSb attracted considerable attention on both experimental measurements and theoretical calculations [12–23]. Due

to the complexity of phase transition, [12] our group adopted a two-step ball milling and quick hot press process to successfully fabricate nanostructured MgAgSb materials without impurity [13–15,21,23], which showed a record high conversion efficiency of 8.5% with a single thermoelectric leg based on operating between 293 K and 518 K [16]. Nevertheless, there is as yet no report on the mechanical properties of nanostructured α -MgAgSb.

In the present study, we thoroughly investigated the mechanical properties of nanostructured α -MgAgSb. It exhibits a Young's modulus of 55.0 GPa, a nanoindentation hardness of 3.3 GPa, a compressive strength of 389.6 MPa, and fracture toughness of 1.1 MPa m^{1/2}. The good mechanical properties of nanostructured α -MgAgSb further demonstrate the excellent potential of this material for heat harvesting.

Experimental procedures for sample preparation and microstructural characterization of nanostructured α -MgAgSb alloy have already been given in our earlier papers [21,23]. Nanoindentation experiments were carried out with the Berkovich diamond indenter B-L72. Elastic modulus and hardness (nano) were determined from the measured load penetration depth curves under loading/unloading through standard data analysis software. The loading/unloading rate was set to be constant 10 nm s^{−1}. Compression tests were performed for the size of sample $\sim \phi 3 \times 5$ mm³ on Instron 5569 testing system at a crosshead displacement speed of 0.5 mm/min. Fracture toughness measurements were carried out employing the indentation-crack technique using Vickers micro-hardness tester (Akashi, AAV-502) with a load of 4.9 N for 10 s of indentation time. All the mechanical properties were measured on 3 samples and their average values were finally chosen.

* Corresponding authors.

E-mail addresses: zren@uh.edu (Z. Ren), suijiehe@hit.edu.cn (J. Sui).

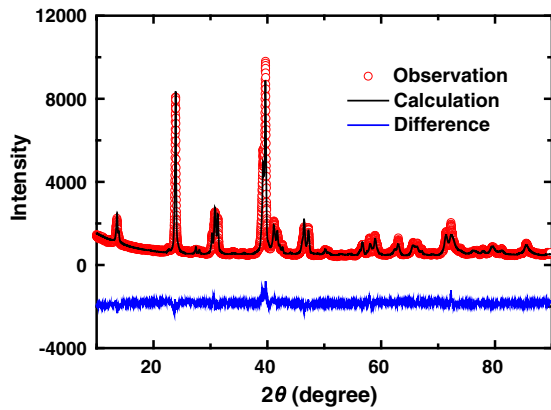


Fig. 1. X-ray diffraction (XRD) pattern with corresponding Rietveld refinement of hot pressed nanostructured MgAgSb alloy.

Fig. 1 shows the XRD pattern with the corresponding Rietveld refinement using the Fullprof software for hot pressed MgAgSb sample. All the diffraction peaks are well fitted with α -MgAgSb (space group $I\bar{C}42$) without any impurity phase within the detection limit of the XRD spectrometer [12]. **Fig. 2** presents the thorough microstructural characterization of nanostructured MgAgSb using SEM, TEM, and HRTEM. **Fig. 2a** shows the clear characteristic of intergranular brittle fracture without any observable micro-hole. Since mechanical properties are extremely sensitive to the porosity, high relative density could guarantee the optimum mechanical properties. The average grain size is only around 150 nm, much smaller than that of nanostructured BiSbTe and CoSb₃ skutterudites alloys [24,25]. This can be ascribed to the observably low hot press temperature (573 K) that does not lead to the obvious grain-coarsening phenomenon during hot press process. **Fig. 2b** shows the clear grain boundary that demonstrates the highly crystallized nature

of nanostructured α -MgAgSb. More importantly, nanoinclusions ranging from 10 to 30 nm could be clearly observed, as indicated in **Fig. 2c**. **Fig. 2d** shows the typical morphology of nanoinclusion that possesses slightly different crystalline orientation and interatomic distance with surrounding grains. The high density of boundaries and interfaces play a critical role in the following the mechanical properties [26–28].

Fig. 3 presents the room temperature hardness and strength of nanostructured MgAgSb. The typical load-displacement nano-indentation curve is shown in the **Fig. 3a**. Since the measured results are somewhat dependent on the load value, high load value normally will guarantee the accuracy and validity [29]. Therefore, a maximum load of around 232 mN is chosen with 10 s holding, much larger than that of other reports [9,11,30], and the corresponding displacement is about 2070 nm. Using the method developed by Oliver and Pharr [31], the derived Young's modulus and hardness are 55.0 GPa and 3.3 GPa, respectively. Young's modulus is a measure of the stiffness of linear elastic solid materials. It is mainly dominated by the strength of chemical bonding on the microscopic level [32], thus not very sensitive to micro-structure. Due to the intrinsic weak bonding of Ag–Sb [22], the Young's modulus of MgAgSb is similar with that of p-type Bi_{0.4}Sb_{1.6}Te₃ (~41.5 GPa) [30] and II–VI compounds materials (PbTe ~ 45.4 GPa [33], PbSe ~ 62.6 GPa [34], and SnTe ~ 64.3 GPa [35]), but much lower than that of p-type nanostructured Mn_{0.9}Fe_{3.1}Co_{0.9}Sb₁₂ (~120 GPa) [36]. Nevertheless, the hardness of MgAgSb is almost comparable with that of p-type skutterudites Mn_{0.9}Fe_{3.1}Co_{0.9}Sb₁₂ (~4.2 GPa) [36], significantly higher than that of p-type Bi_{0.4}Sb_{1.6}Te₃ (~1.1 GPa) [30] and II–VI compounds (PbTe ~ 0.4 GPa [33], PbSe ~ 0.44 GPa [34], and SnTe ~ 0.65 GPa [35]). **Fig. 3d** presents the typical compressive stress-strain curve at room temperature under uniaxial compressive loading. This curve shows a representative brittle fracture feature, consistent with the fracture morphology in **Fig. 2a**. The corresponding compressive strength is around 389.6 MPa, much higher than that of p-type Bi_{0.5}Sb_{1.5}Te₃ (~110 MPa) [37], PbTe (~122 MPa) [38], and Cu₂Se (~140 MPa) [39]. The good mechanical performance, including high

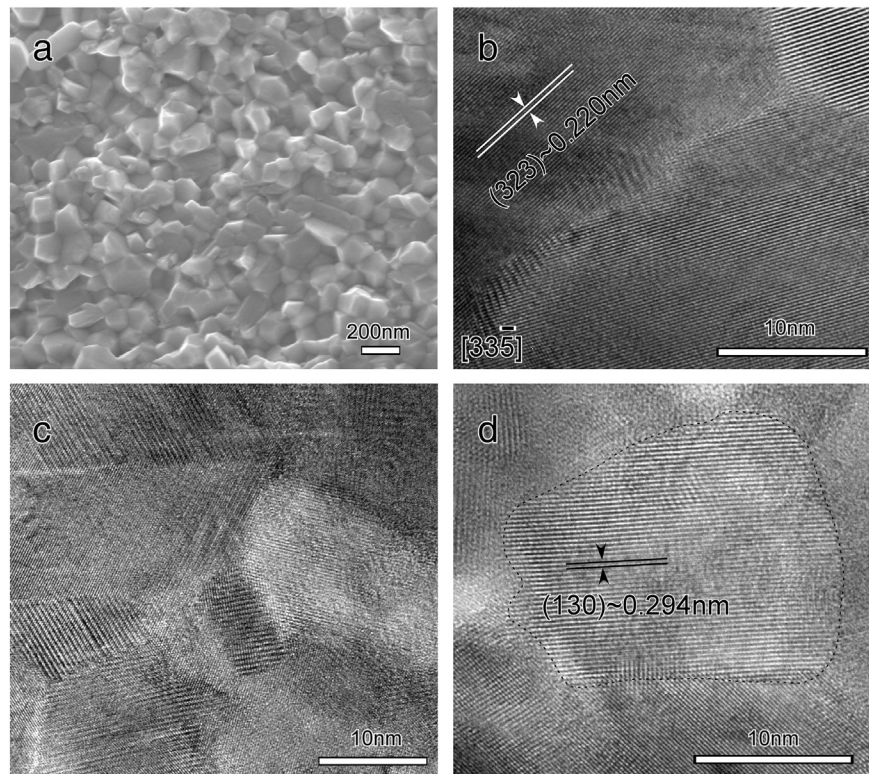


Fig. 2. Microstructural characterization of nanostructured MgAgSb alloy. (a) Scanning electron microscope (SEM) image showing the average grain size; (b) high magnification TEM (HRTEM) image of the grain boundary showing good crystallization; (c) HRTEM image showing nano-scale special feature; (d) HRTEM image showing a typical nanoinclusion morphology.

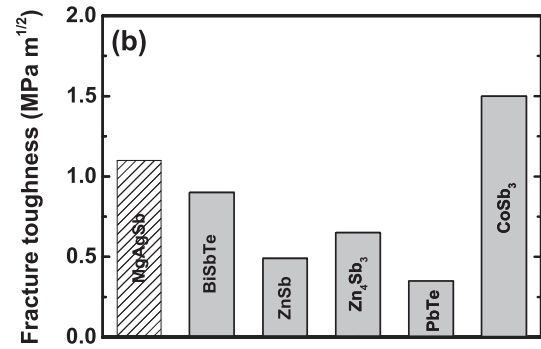
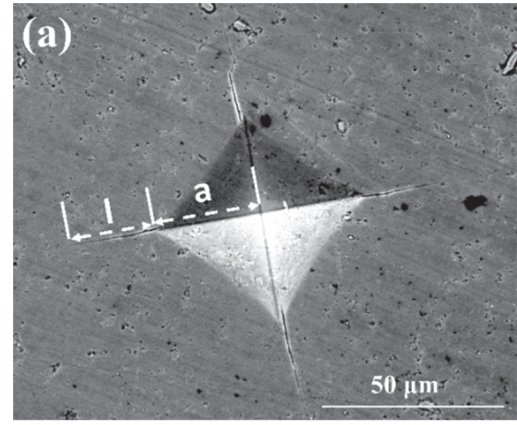
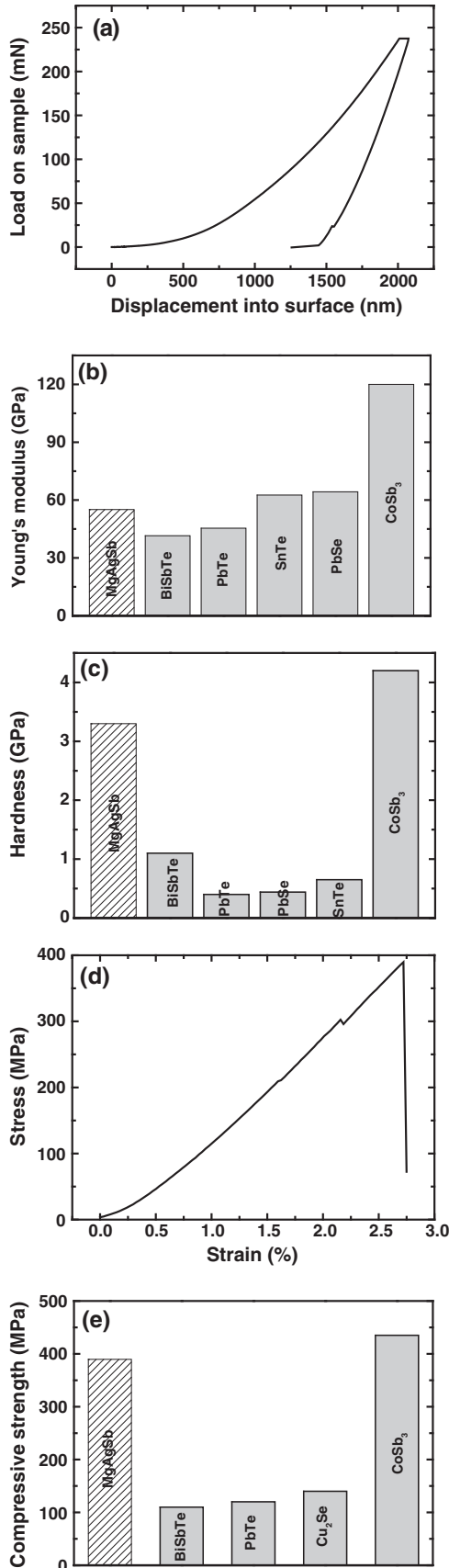


Fig. 4. (a) SEM image of Vickers indentation of nanostructured MgAgSb alloy with marked indentation crack length l and the half-diagonal of indentation a ; (b) the calculated fracture toughness in comparison with other p-type low and medium temperature thermoelectric materials [9,38,44–46].

hardness and strength, is possibly related with grain boundary hardening (or strengthening) effect [26–28], benefiting from grain refinement for nanostructured MgAgSb. As known, grain refinement could significantly enhance the hardness and strength for nanostructured metals and alloys based on empirical Hall-Petch relation [40,41], $\sigma_y = \sigma_0 + k_1 d^{1/2}$, where σ_y , σ_0 , k_1 , and d are the yield stress, materials constant, strengthening coefficient, and average grain diameter, respectively. This effect is a consequence of dislocation pile-ups at the grain boundaries and interfaces in nanostructured materials [26]. Besides, precipitation hardening (or strengthening) by nanoprecipitates, acting as localized obstacles to dislocation propagation [26], may also play a vital role in the good mechanical performance. However, it is difficult to quantitatively separate the contribution of hardening (or strengthening) effect by grain boundaries or nanoprecipitates in the present work.

To evaluate the ability of brittle materials containing a crack to resist fracture, here fracture toughness (K_{IC}) is measured by Vickers indentation-crack technique according to the method proposed by Niihara et al. [42],

$$K_{IC} = 0.0089 \left(\frac{E}{HV} \right)^{2/5} \times \frac{P}{a l^{1/2}}, 0.25 \leq \frac{l}{a} \leq 2.5$$

where E is the Young's modulus (GPa), HV is the Vickers hardness (GPa), P is the load (Newtons), a is the half-diagonal of Vickers indentation (meters), and l is the crack length (meters) on the material surface

Fig. 3. (a) The typical load-displacement nano-indentation curve of nanostructured MgAgSb alloy; (b) and (c) the derived Young's modulus and hardness in comparison with other p-type low and medium temperature thermoelectric materials, respectively [31,34–36]; (d) the typical compressive stress-strain curve of nanostructured MgAgSb alloy at room temperature under uniaxial compressive loading; (e) The corresponding compressive strength in comparison with other p-type low and medium temperature thermoelectric materials [9,38–40].

after indenter removal. The measured Vickers hardness is 2.9 GPa, comparable with nanoindentation hardness (3.3 GPa) within the experimental error for brittle materials [29]. The calculated fracture toughness (Fig. 4) of nanostructured MgAgSb is relatively high ($\sim 1.1 \text{ MPa m}^{1/2}$), in comparison with that of p-type thermoelectric materials such as $\text{Bi}_{0.5}\text{Sb}_{1.5}\text{Te}_3$ ($\sim 0.9 \text{ MPa m}^{1/2}$) [37], ZnSb ($\sim 0.5 \text{ MPa m}^{1/2}$) [43], Zn_4Sb_3 ($\sim 0.6 \text{ MPa m}^{1/2}$) [44], $\text{Pb}_{0.95}\text{Sn}_{0.05}\text{Te-PbS}$ 8% ($\sim 0.3 \text{ MPa m}^{1/2}$) [45], and $\text{Mm}_{0.78}\text{Fe}_3\text{CoSb}_{12}$ ($\sim 1.5 \text{ MPa m}^{1/2}$) [7]. The good toughness behavior of nanostructured MgAgSb indicates a combination of high strength and ductility, which may be related with toughening mechanisms via the intricate microstructure [46]. Those high density of boundaries and interfaces lead to crack bifurcation and deflection and thus contributes to the dissipation of energy during crack propagation [46].

In summary, the mechanical properties of nanostructured MgAgSb are systematically investigated using nano-indentation, uniaxial compressive loading, and Vickers indentation-crack measurements. The corresponding Young's modulus, nanoindentation hardness, compressive strength, and fracture toughness are 55.0 GPa, 3.3 GPa, 389.6 MPa and $1.1 \text{ MPa m}^{1/2}$, respectively, as a direct result of the nanostructure nature. Compared with other p-type state-of-the-art thermoelectric materials, the good mechanical properties coupled with high thermoelectric performance indicate that p-type nanostructured MgAgSb is a good candidate for power generation application in the low temperature range.

Acknowledgements

The work performed at the University of Houston was funded by the US Department of Energy under Contract Number DOE DE-SC0010831 (sample preparation and characterizations); and by the National Natural Science Foundation of China (no. 51471061 and 512710699) (mechanical property test).

References

- [1] M.S. Dresselhaus, G. Chen, M.Y. Tang, R. Yang, H. Lee, D. Wang, Z. Ren, J.P. Fleurial, P. Gogna, *Adv. Mater.* 19 (2007) 1043–1053.
- [2] W. Liu, Q. Jie, H.S. Kim, Z. Ren, *Acta Mater.* 87 (2015) 357–376.
- [3] W. Liu, H.S. Kim, Q. Jie, Z. Ren, *Scr. Mater.* 111 (2016) 3–9.
- [4] J. Yang, F.R. Stabler, *J. Electron. Mater.* 38 (2009) 1245–1251.
- [5] Y. Pei, H. Wang, G. Snyder, *Adv. Mater.* 24 (2012) 6125–6135.
- [6] Y. Lan, A.J. Minnich, G. Chen, Z. Ren, *Adv. Funct. Mater.* 20 (2010) 357–376.
- [7] G. Rogl, P. Rogl, *Sci. Adv. Mater.* 3 (2011) 517–538.
- [8] S. Bathula, B. Gahtori, M. Jayasimhadri, S. Tripathy, K. Tyagi, A. Srivastava, A. Dhar, *Appl. Phys. Lett.* 105 (2014) 061902.
- [9] G. Rogl, A. Grytsiv, M. G rth, A. Tavassoli, C. Ebner, A. W nschek, S. Puchegger, V. Soprunyuk, W. Schranz, E. Bauer, *Acta Mater.* 107 (2016) 178–195.
- [10] S. Gahlawat, R. He, S. Chen, L. Wheeler, Z. Ren, K. White, *J. Appl. Phys.* 116 (2014) 083516.
- [11] R. He, S. Gahlawat, C. Guo, S. Chen, T. Dahal, H. Zhang, W. Liu, Q. Zhang, E. Chere, K. White, *Phys. Status Solidi A* 212 (2015) 2191–2195.
- [12] M.J. Kirkham, A.M. dos Santos, C.J. Rawn, E. Lara-Curzio, J.W. Sharp, A.J. Thompson, *Phys. Rev. B* 85 (2012) 144120.
- [13] H. Zhao, J. Sui, Z. Tang, Y. Lan, Q. Jie, D. Kraemer, K. McEnaney, A. Guloy, G. Chen, Z. Ren, *Nano Energy* 7 (2014) 97–103.
- [14] J. Shuai, H.S. Kim, Y. Lan, S. Chen, Y. Liu, H. Zhao, J. Sui, Z. Ren, *Nano Energy* 11 (2015) 640–646.
- [15] J. Sui, J. Shuai, Y. Lan, Y. Liu, R. He, D. Wang, Q. Jie, Z. Ren, *Acta Mater.* 87 (2015) 266–272.
- [16] D. Kraemer, J. Sui, K. McEnaney, H. Zhao, Q. Jie, Z. Ren, G. Chen, *Energy Environ. Sci.* 8 (2015) 1299–1308.
- [17] P. Ying, X. Liu, C. Fu, X. Yue, H. Xie, X. Zhao, W. Zhang, T. Zhu, *Chem. Mater.* 27 (2015) 909–913.
- [18] N. Miao, P. Ghosez, *J. Phys. Chem. C* 119 (2015) 14017–14022.
- [19] C. Sheng, H. Liu, D. Fan, L. Cheng, J. Zhang, J. Wei, J. Liang, P. Jiang, J. Shi, *J. Appl. Phys.* 119 (2016) 195101.
- [20] N. Miao, J. Zhou, B. Sa, B. Xu, Z. Sun, *Appl. Phys. Lett.* 108 (2016) 213902.
- [21] Z. Liu, Y. Wang, J. Mao, H. Geng, J. Shuai, Y. Wang, R. He, W. Cai, J. Sui, Z. Ren, *Adv. Energy Mater.* 6 (2016) 1502269.
- [22] D. Li, H. Zhao, S. Li, B. Wei, J. Shuai, C. Shi, X. Xi, P. Sun, S. Meng, L. Gu, *Adv. Funct. Mater.* 25 (2015) 6478–6488.
- [23] Z. Liu, J. Shuai, J. Mao, Y. Wang, Z. Wang, W. Cai, J. Sui, Z. Ren, *Acta Mater.* 102 (2016) 17–23.
- [24] Y. Lan, B. Poudel, Y. Ma, D. Wang, M.S. Dresselhaus, G. Chen, *Nano Lett.* 9 (2009) 1419–1422.
- [25] Q. Jie, H. Wang, W. Liu, H. Wang, G. Chen, Z. Ren, *Phys. Chem. Chem. Phys.* 15 (2013) 6809–6816.
- [26] H. Gleiter, *Acta Mater.* 48 (2000) 1–29.
- [27] C. Koch, *Scr. Mater.* 49 (2003) 657–662.
- [28] K. Lu, *Nature Reviews Materials* 1 (2016) 16019.
- [29] L. Qian, M. Li, Z. Zhou, H. Yang, X. Shi, *Surf. Coat. Technol.* 195 (2005) 264–271.
- [30] G. Li, K. Gadelrab, T. Souier, P.L. Potapov, G. Chen, M. Chiesa, *Nanotechnology* 23 (2012) 065703.
- [31] W.C. Oliver, *J. Mater. Res.* 7 (1992) 1564–1583.
- [32] D.J. Green, *An Introduction to the Mechanical Properties of Ceramics*, Cambridge University Press, 1998.
- [33] B. Li, P. Xie, S. Zhang, D. Liu, *J. Mater. Sci.* 46 (2011) 4000–4004.
- [34] R.D. Schmidt, E.D. Case, L.-D. Zhao, M.G. Kanatzidis, *J. Mater. Sci.* 50 (2015) 1770–1782.
- [35] R.D. Schmidt, E.D. Case, J.E. Ni, R.M. Trejo, E. Lara-Curzio, R.J. Korkosz, M.G. Kanatzidis, *J. Mater. Sci.* 48 (2013) 8244–8258.
- [36] T. Dahal, S. Gahlawat, Q. Jie, K. Dahal, Y. Lan, K. White, Z. Ren, *J. Appl. Phys.* 117 (2015) 055101.
- [37] Y. Zheng, Q. Zhang, X. Su, H. Xie, S. Shu, T. Chen, G. Tan, Y. Yan, X. Tang, C. Uher, *Adv. Energy Mater.* 5 (2015) 1401391.
- [38] Y. Gelbstein, G. Gotesman, Y. Lishzinker, Z. Dashevsky, M. Dariel, *Scr. Mater.* 58 (2008) 251–254.
- [39] K. Tyagi, B. Gahtori, S. Bathula, M. Jayasimhadri, S. Sharma, N.K. Singh, D. Haranath, A. Srivastava, A. Dhar, *Solid State Commun.* 207 (2015) 21–25.
- [40] N. Petch, *J. Iron Steel, Inst.* 174 (1953) 25–28.
- [41] E. Hall, *Section B* 64 (1951) 747.
- [42] K. Niihara, R. Morena, D. Hasselman, *J. Mater. Sci. Lett.* 1 (1982) 13–16.
- [43] F. Tseng, S. Li, C. Wu, Y. Pan, L. Li, *J. Mater. Sci.* 51 (2016) 5271–5280.
- [44] K. Ueno, A. Yamamoto, T. Noguchi, T. Inoue, S. Sodeoka, H. Obara, *J. Alloys Compd.* 388 (2005) 118–121.
- [45] J.E. Ni, E.D. Case, K.N. Khabir, R.C. Stewart, C.-I. Wu, T.P. Hogan, E.J. Timm, S.N. Girard, M.G. Kanatzidis, *Mater. Sci. Eng. B* 170 (2010) 58–66.
- [46] P.F. Becher, *J. Am. Ceram. Soc.* 74 (1991) 255–269.